THE STRUCTURE OF NGC 7027 AND A DETERMINATION OF ITS DISTANCE BY MEASUREMENT OF PROPER MOTIONS

COLIN R. MASSON
California Institute of Technology
Received 1988 March 11; accepted 1988 June 21

ABSTRACT

We present new VLA maps of the planetary nebula NGC 7027, with a resolution of 0″.35. These maps show extreme limb brightening, with a limb/center contrast of 6:1, which cannot be reproduced by models which represent the nebula as a homogeneous shell, but can be explained by a new model which takes into account inverse-square law dilution of ionizing radiation from the central star. The structure of NGC 7027 is well represented by an elongated, ellipsoidal shell tilted at 30° to the line of sight. In an end-on view of such an elongated shell, the central surface brightness is diminished relative to the limbs because there is less ionized gas at the ends of the shell.

To continue our measurement of angular expansion in this nebula, we have made a third epoch map at 1″.05 resolution. Comparison of this with the earlier two epochs confirms the expansion previously reported and demonstrates that it proceeds at a steady rate. By combining the measured angular expansion with velocity information we deduce that the distance to NGC 7027 is 880 ± 150 pc. A careful analysis of errors shows that the uncertainty arises almost equally from inaccuracy in the model of the nebula, possible luminosity variation in the central star, and measurement errors. Future observations will put a strong limit on the luminosity variations and improve the expansion measurement, giving an ultimate accuracy of better than 10% for the distance measurement, limited chiefly by modeling of the nebular evolution. With this method it should be possible to measure distances to several dozen of the brightest planetary nebulae and to study the evolution of other celestial objects.

Subject headings: nebulae: individual (NGC 7027) — nebulae: internal motions — nebulae: planetary

I. INTRODUCTION

Knowledge of the distance to a planetary nebula is fundamental to the determination of many of its physical properties, such as the luminosity of the central star and the mass of material contained within the ionized region. In general, the distances are poorly determined, since the nebulae have no standard properties which can be used for comparison. For this reason, good distances are available for only a small fraction of the known nebulae. For investigations which require large samples of nebulae, it is necessary to use distance estimates which rely on an assumption that all nebulae are equal in some respect, such as the mass of ionized material. This is a limitation on investigations such as those of Schneider and Terzian (1983) which use planetary nebulae to trace the Galactic rotation curve, or studies which attempt to measure the effect of planetary nebulae on the interstellar medium (e.g., Salpeter 1978). Any method which determines accurate distances to the nebulae is thus important for global studies of the Galaxy as well as for understanding of the last phase of stellar evolution.

In a previous paper (Masson 1986, hereafter Paper I), we presented the first direct radio measurement of angular expansion motions in the planetary nebula NGC 7027, using VLA[1] maps with a resolution of 1″, at epochs separated by only 2.8 yr. This measurement was used, in combination with Doppler data on the velocity of the gas, to deduce the distance to the nebula. The principal source of uncertainty in the calculation

of the distance was the lack of a good model of the nebular structure. Because of the large limb brightening, it was simply assumed in Paper I that the nebula was a thin shell. To improve upon the earlier measurement a more accurate model is required, as well as a longer time interval for the expansion measurement.

Detailed, quantitative modeling of particular nebulae has not often been attempted, probably due to the complexity of their structures. NGC 7027 is a young planetary nebula, whose ionized gas lies in a hollow shell on the inside of a massive neutral cloud (Mufson *et al.* 1975; Masson *et al.* 1985). The whole structure is expanding at a velocity of about 17 km s⁻¹. With the recent availability of high-quality radio maps, several models of NGC 7027 have been made (Scott 1973; Atherton *et al.* 1979; Basart and Daub 1987; Roelfsma *et al.* 1987). All of these models were based on maps with beam sizes of at least 1″, which could not resolve the limbs of the nebula. Therefore, to determine the structure of the nebula we have made VLA maps with 0″.35 resolution, at a frequency of 14.965 GHz, where the emission is optically thin.

To improve upon our previous angular expansion measurement, we have made 4.885 GHz measurements at a third epoch. Because the expansion involved is very small, ∼4 mas yr⁻¹, the changes of structure are unresolved at an angular resolution of 1″ and a very careful comparison of the maps from different epochs is needed to reveal them. In addition, because the changes are not resolved by the 1″ beam, interpretation is a tricky matter and involves consideration of the bulk motion of the gas and the behavior of the ionization front. The new model of the nebula is used to investigate these effects and compare the results with the VLA maps to calculate an improved estimate of the distance to the nebula.

---

[1] The VLA is a facility of the National Radio Astronomy Observatory, which is operated by Associated Universities, Inc., under contract with the National Science Foundation.

II. OBSERVATIONS

The data presented in Paper I consisted of 4.885 GHz maps made with the VLA in B array, during 1982 August (Basart and Daub 1987) and 1985 May. Further 4.885 GHz observations presented here were made in 1986 September, also in B array. In 1985, additional observations were made at a frequency of 14.965 GHz, where the angular resolution of the B array is 0″.35. Each observation was spread over a full 12 hr to obtain good *uv* coverage, but other objects and frequencies were interleaved so the total time on source ranged from 1.5 to 3 hr. The data quality was good, but self-calibration was necessary, as usual, to obtain the best dynamic range. Because of limited computer time, only one of the two IF bands was analyzed.

III. RESULTS

a) Nebular Expansion

To determine the change in the appearance of NGC 7027 due to expansion, the three epochs of 4.885 GHz data were treated according to the prescription of Paper I to obtain difference maps for the time intervals 1982–1985 and 1982–1986. A full discussion of the technique is given in Paper I, but we summarize it briefly here for completeness. Since the changes in size between any two epochs are very small, amounting to less than 1% of the radius, it is necessary to make a very careful comparison to reveal them. There are two principal sources of error, calibration errors and differences in synthesized beam shape between the two epochs. Both of these smear the two maps differently and would give rise to spurious apparent changes if the two maps were just crudely subtracted. The calibration errors at one epoch can be almost eliminated by the process of self-calibration (Schwab 1980). This is an iterative procedure in which the map itself is fitted to the observations to determine the calibration errors and so produce a new, more accurate map. The process converges because the 351 interferometer pairs of the VLA are subject to only 27 calibration scale factors, one per antenna. To ensure that any residual calibration errors are the same for both epochs, a cross-calibration step is then used, in which the penultimate map from the self-calibration process is used as the model for calibrating the data from the other epoch. Any (small) beam smearing due to imperfect calibration should then become the same at the two epochs. The difference in beam shapes between the two epochs is taken care of by using the CLEAN deconvolution algorithm to generate a deconvolved model of the map from one epoch and then subtracting this model from the cross-calibrated visibility data from the other epoch. Differences in beam shape arise from different coverage in the *uv* plane, and this procedure is equivalent to an interpolation from the *uv* points measured at one epoch to the (nearby) points measured at the other, followed by subtraction. Finally, the subtracted visibility data are Fourier-transformed to produce a map of the difference in source appearance between the two epochs, convolved with the beam shape appropriate for the second epoch.

In both difference maps there was a noticeable asymmetry, largely along the major axis of the nebula. This effect is also present in the difference map presented in Paper I and is apparently due to a small misregistration of the two maps. The cause of this misregistration is not known, but it is probably due to a computational problem. In principle, the cross-calibration step should align the two data sets, but the perfection of this alignment may be marred by the differences in structure due to the expansion of the source. The asymmetry was removed by making small shifts in the relative positions of the maps before subtraction. The required position shifts were 8 mas for the 1982–1985 map and 20 mas for the 1982–1986 map.

Flux density measurements at the VLA do not have enough precision to determine the amplitude scales absolutely, so we chose the amplitude scaling to set the integrated flux density of the difference map to zero. Since the nebula is nearly optically thin at 4.885 GHz, this is approximately correct if the ionizing luminosity of the central star remains constant and, in any case, provides a well-determined scaling for comparison with models. After CLEANing, the difference maps were restored with a 1″.05 diameter circular Gaussian beam.

Figure 1 shows the final two difference maps, along with the 1986 epoch map which has also been CLEANed and restored with a 1″.05 beam. Because the nebula has the appearance of a ring, the difference due to an expansion should be a very thin negative ring at the outside of the nebula and a very thin positive ring at the inside edge. Before convolution with the beam, these rings have brightnesses comparable with the peak brightness on the single epoch map and widths much narrower than the beam. Convolution with the beam smears out the difference map, giving negative and positive rings with an apparent width ~1″ and with amplitudes proportional to the unconvolved widths. The magnitude of the expansion is thus shown by the peak intensity on the difference map and not by the widths or locations of the rings. The difference maps in Figure 1 are plotted with contour intervals proportional to the time interval between the epochs (2.8 and 4.1 yr, respectively) so that a difference due to steady expansion should give the same number of contours in the two maps. It is immediately apparent from the close similarity of the two difference maps that the new epoch shows a steady continuation of the expansion. This confirms that the original result (Paper I) was due to a real change in the source and demonstrates that the change is continuing at a nearly constant rate.

Several different methods were considered for determining the magnitude of the expansion. Of these, the simplest and most robust was the method used in Paper I, in which the peaks of the difference map were compared with the gradients at the appropriate positions on the epoch 1986 map. As before, we have analyzed only the minor axis, since the ends of the major axis have a more complex structure. To determine the peaks of the difference maps and the gradients on the 1986 map, three cuts were made in p.a. 56° passing near the map center. The values from opposite sides of the map were averaged to avoid problems due to misregistration. Table 1 lists the values of slopes and peak differences, while Figure 2 shows a plot of peak difference against time. For both the positive and negative peaks, we calculated a weighted average ratio of peak difference divided by time. These average ratios are shown by the lines plotted in Figure 2. This figure shows that there is a nearly linear relation between peak differences and time. The small deviation from linearity apparent in the plots in Figure 2 is also visible in the maps in Figure 1. With only two measurements, it is hard to tell whether this deviation is real or whether it is due to some artifact of the data reduction. We base our measurement on the outer peak of the difference map since it is better defined than the inner one and less sensitive to scaling errors in the subtraction. A simple calculation based on the values in Table 1 indicates that the apparent motion of the ionized gas is 4.37 ± 0.35 mas yr^{-1}. The quoted error is a
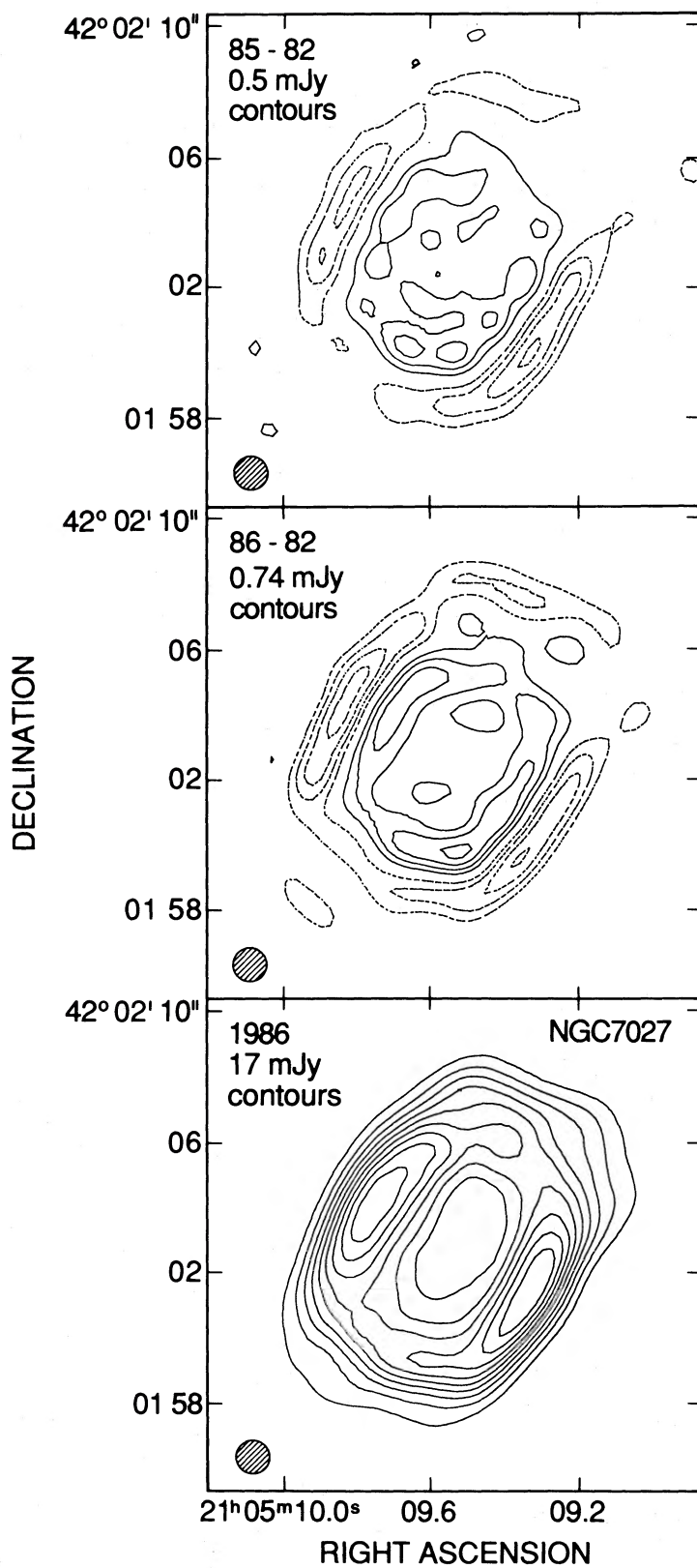
Fig. 1.—Difference maps showing the change of NGC 7027 over intervals of (*top*) 2.8 and (*middle*) 4.1 yr. The contour levels are 0.5, 1.0, 1.5, 2.0, 2.5, and 3.0 mJy per beam in the first case, and a factor of (4.1/2.8) greater in the second. The similarity of the two maps indicates therefore that the source is changing at a steady rate. The restoring beam was Gaussian with a FWHM of 1".05. (*bottom*) Map of NGC 7027 at 1985 May 21 with a resolution of 1".05. The contour interval is 10% of the peak intensity of 170 mJy beam^{-1}. The shaded ellipses show the FWHM beam areas.

296

TABLE 1

VALUES OF SLOPES AND PEAK DIFFERENCES

Epoch	Outer Peak (mJy)	Inner Peak (mJy)	Outer Gradient (mJy arcsec^{-1})	Inner Gradient (mJy arcsec^{-1})
85–82	-1.67 ± 0.12	1.31 ± 0.11	...	...
86–82	-2.80 ± 0.17	2.49 ± 0.13	...	...
86	...	...	147 ± 9	86 ± 4

formal one, based on the scatter among the measurements of the peak differences and the map gradients. A correction is required to obtain the physical motion of the gas. This is calculated below from a model of the nebula.

b) 2 Centimeter Maps

With a beamwidth of 1″05 at 4.885 GHz, the nebular structure is barely resolved so measurements were made at 14.965 GHz to obtain higher resolution. The data from 1985 May were used, and the resulting map is shown in Figure 3. After two cycles of self-calibration, the resulting map was CLEANed with the MX program and restored with an elliptical Gaussian beam of 0″35 × 0″34 diameter. At a frequency of 14.965 GHz, the nebula is entirely optically thin and the structure is well-resolved. The nebula is strongly limb brightened in all directions indicating that it has the form of a closed hollow shell. An asymmetric, open toroidal structure could produce the same appearance, but only if it was fortuitously arranged so that its

axis was well-aligned with the line of sight. The nebula is significantly asymmetrical at this high resolution, with the two sides of the minor axis differing in peak intensity by 1.3:1. For the sake of modeling, we adopt an average value of 28 mJy per beam for the minor axis peak and 4.3 mJy per beam for the center, giving a large contrast of 6.4. The lack of short spacing information may have depressed the center relative to the limbs, but this effect is unlikely to reduce the contrast ratio much below 6.0. The limbs are well-resolved, with widths at half-power of 1″3 and 2″0 for the SW and NE sides, respectively.

To a first approximation the nebula has an elliptical shape, although there are significant deviations, particularly in the lowest contours. Figure 4 shows the 4.885 GHz map from Figure 2, but plotted with logarithmic contours to emphasize the low-level features. The outer boundary is more like a parallelogram, with narrow extensions to the northwest and southeast. These extensions, which are symmetrical about the
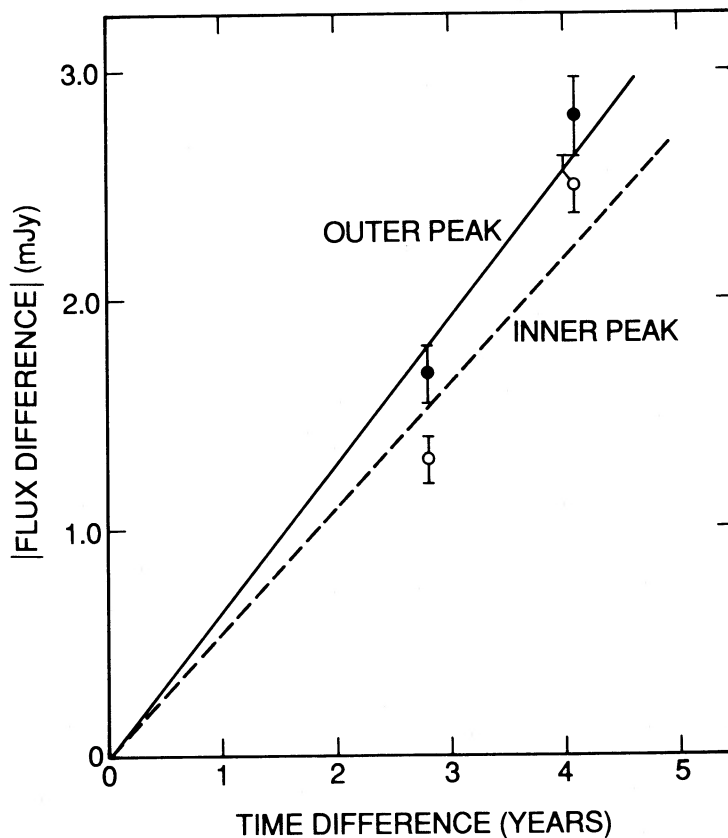

FIG. 2.—Graph of the peak differences against time. The filled circles and solid line refer to the outer peak, while the open circles and dashed line refer to the inner peak.
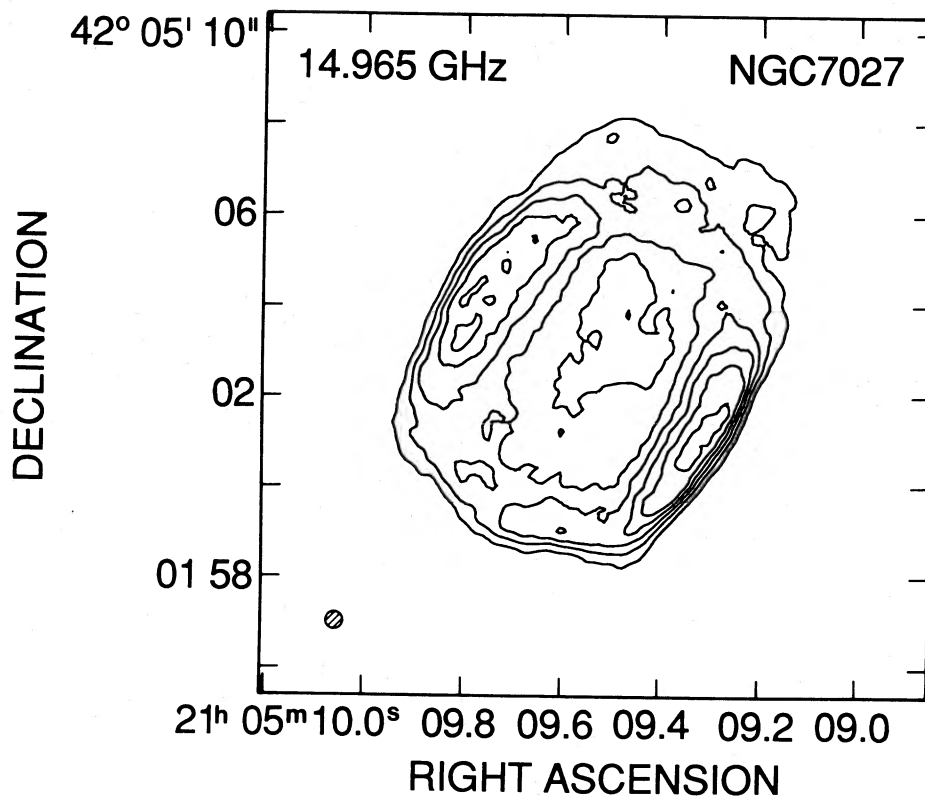
FIG. 3.—High-resolution map of NGC 7027 at 14.965 GHz. The restoring beam was $0''35 \times 0''34$ FWHM. The contour interval is 10% of the peak intensity of 32.7 mJy beam^{-1}. The shaded ellipse shows the FWHM beam area.

center of the nebula resemble the ansae seen in some other nebula (e.g., Phillips, Reay, and Worswick 1980). In the case of a nebula like NGC 7027, which is completely surrounded by neutral gas, such extensions must indicate regions of low density in the neutral gas, which allow the ionization front to expand farther.

IV. THE STRUCTURE OF THE NEBULA

Four previous investigations have sought to determine the detailed three-dimensional structure of NGC 7027. Basart and Daub (1987) compared maps at different radio frequencies to calculate the distribution of temperature and optical depth across the face of the nebula. Scott (1973) showed that a low-resolution radio map was well represented by a uniform cylinder with $1''2$ thick walls, whose major axis was inclined at $30°$ to the line of sight. Atherton et al. (1979) presented a model with a more realistic closed ellipsoidal shell structure, with a minor axis thickness of $0''6$, inclined at $34°$ to the line of sight. In their model, large temperature and density variations were invoked, with the largest densities and temperatures being found on the inner edge of the minor axis. The details of this model appear to be contradicted by our new 14.965 GHz map, which shows that the strongest emission occurs at the outer edge of the minor axis, and that the limbs have a thickness of $1''6$ FWHM. More recently Roelfsma et al. (1988) found that their velocity data were well-fitted by simple velocity fields in a prolate spheroidal shell of ionized gas, with a thickness of $0''6$, and an inclination of $40°$ to the line of sight.

There are many possible free parameters in a general model of the nebular structure. We have sought to minimize these by

assuming constant temperature and density since there is little direct evidence for large variations of these quantities in the bulk of the gas. We have also added one important physical constraint, ignored in previous modeling, which is that the optically thin radio flux in any part of the nebula is proportional to the local flux of ionizing radiation (Masson 1989a). Therefore regions of the nebula which are close to the star must produce more radio flux than those which are farther away. This simple relation provides a powerful constraint on nebular models, as well as explaining the paradoxically large limb/center contrast in our 14.965 GHz map. It is easy to show that a homogeneous spherical or elliptical shell of radius r and thickness t will have a limb/center contrast of $(2r/t - 1)^{1/2}$. In the case of NGC 7027, the contrast ratio of 6.4 would require a thickness of $0''2$, in gross conflict with our measured limb width of $1''6$. The solution to this dilemma is found in the fact that a homogeneous nebula could not be maintained in ionization by a single central source. Because of the dependence of ionization on local radiation, there is less emission from the ends of an elongated shell since they are farther from the ionizing star. When such an elongated structure is viewed nearly end-on, the line of sight passing through the center of the nebula pierces the shell near the ends, where there is much less emission than in a uniform shell. Thus the limb/center contrast is increased without requiring a thin shell.

The model for NGC 7027 consists of ionized gas at a uniform temperature of 14,500 K (Roelfsma et al. 1988), distributed in a region bounded by two prolate ellipsoids of revolution. The difference between the major radii is equal to the difference between the minor radii so that the shell has a
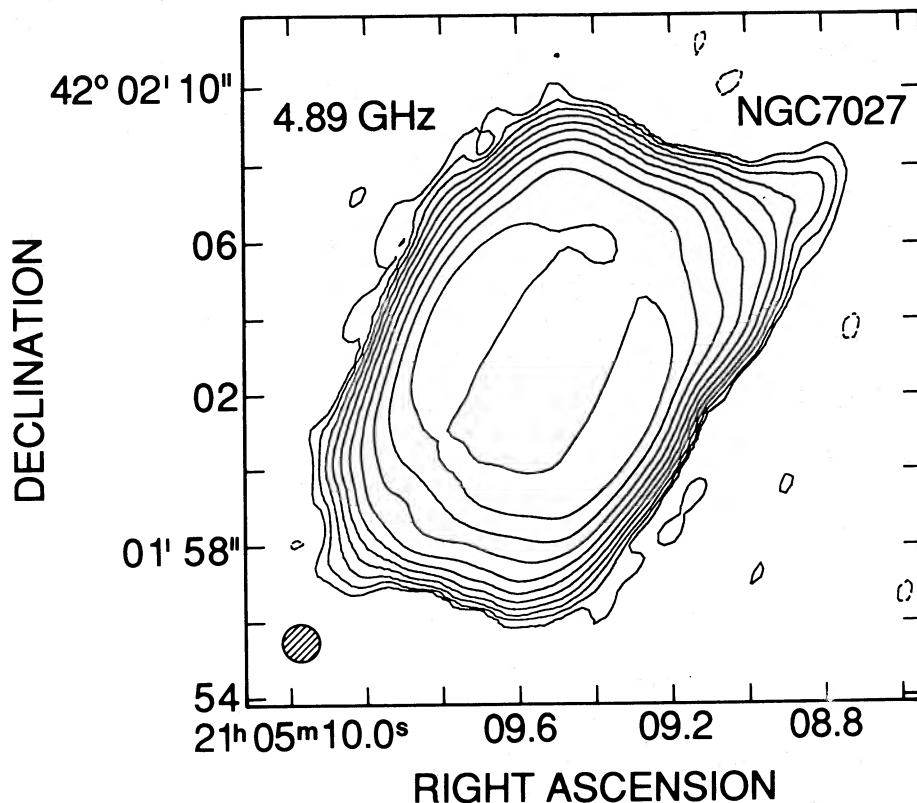
FIG. 4.—Map of NGC 7027 at 4.885 GHz with logarithmic contours to emphasize low-level features. Note the "jets" protruding from the NW and SE corners of the nebula. The restoring beam was 1″05 FWHM, and the contour levels are −0.2, 0.2, 0.4, 0.8, 1.6, 3.2, 6.4, 12.8, 25.6, 51.2, and 102.4 mJy beam^{-1}. The shaded ellipse shows the FWHM beam area.

roughly constant thickness everywhere. To enforce consistency with the ionizing flux constraint, the density of the gas varies inversely with distance to the central star. The emission therefore varies as the inverse square of the distance to the central star. In practice, the model was constructed of a number of nested shells with equal densities along the nebular equator. Within each shell, the density varied inversely with distance to the central star. While this is not a perfectly consistent physical model, it is sufficiently accurate to capture the main physical effects and produce a reasonably realistic nebula (Masson 1989a). As constraints for our model we have used total flux densities at 1.465, 4.885, and 14.965 GHz, the dimensions of the optically thick 1.465 GHz map presented by Basart and Daub (1987), the limb thickness measured at 14.965 GHz, and the intensities of the limb and center of the 14.965 GHz map presented here. These data are gathered in Table 2. The flux densities are taken from the compilation of Baars et al. (1977) since these are the most consistent set. Standard VLA data, for example, are calibrated against other sources listed by Baars et al. and therefore have no greater claim to accuracy.

The calculations were run for models with inclination angles (measured between the major axis of the nebula and the line of sight) of 30°, 35°, and 40°, in the range indicated by previous modeling. The results are tabulated in Table 2 for comparison with the measurements. At any given inclination angle in this range, it was possible to find a fairly good fit to the total flux densities and overall dimensions although the model param-

eters were very tightly constrained by the observations. Models with inclinations of 35° and 40°, however, cannot simultaneously match the large observed limb width and the observed degree of limb brightening. The observed limb width requires that the nebula have a rather thick shell, $\sim 1″3$, which can be consistent with the observations only when viewed at an inclination angle of 30° ± 5°. The best-fitting model is the one at 30° inclination which has fairly thick walls. This is, in fact, quite similar to the original cylindrical model presented by Scott (1973). A model at 25° inclination provided a somewhat worse fit to the data in Table 2 and gave a poorer representation of the appearance at 14.965 GHz. We have not attempted to reproduce the model of Atherton et al. (1979) but we believe that their thin shell (0″6) would conflict with the appearance of the high-resolution 14.965 GHz map in having limbs which are much too narrow. It is interesting to note that the particular variations of density and temperature adopted by Atherton et al. have the effect of reducing emission from the ends of the shell in much the same way that results automatically from the ionizing flux constraint.

As can be seen by comparing the model maps in Figure 5 with those above and with the 1.465 GHz map of Basart and Daub (1987), there are still some deficiencies. The minor axis of the nebula is well modeled but the major axis is inaccurate in two respects. First, the NS brightness asymmetry in the 1.465 GHz map of Basart and Daub obviously cannot be reproduced with any centro-symmetric model with uniform temperature.

<div align="center">

TABLE 2

MODEL CONSTRAINTS

</div>

Parameter	Measured	Model 1	Model 2	Model 3
Inclination angle (degrees)	...	40	35	30
Inner minor radius (arcsec)	...	3.1	2.8	2.5
Outer minor radius (arcsec)	...	3.8	3.8	3.8
Inner axial ratio	...	2.25	2.76	3.43
Outer axial ratio	...	2.0	2.3	2.6
Flux density:				
1.465 GHz (Jy)	1.48 ± 0.03[a]	1.48	1.52	1.52
4.885 GHz (Jy)	5.66 ± 0.11[a]	5.2	5.3	5.5
14.965 GHz (Jy)	6.1 ± 0.125[a]	5.7	5.8	6.1
Minor axis (1.465 GHz) (arcsec)	7.4 ± 0.2[b]	7.6	7.5	7.6
Major axis (1.465 GHz) (arcsec)	11.4 ± 0.2[b]	11.2	11.6	11.4
Minor axis limb width (14.965 GHz) (arcsec)	1.6 ± 0.3	1.0	1.2	1.5
Central intensity (14.965 GHz) (K)	207 ± 30	283	268	256
Limb intensity (14.965 GHz) (K)	1335 ± 200	1370	1303	1264
Correction factor	...	0.96	0.91	0.87

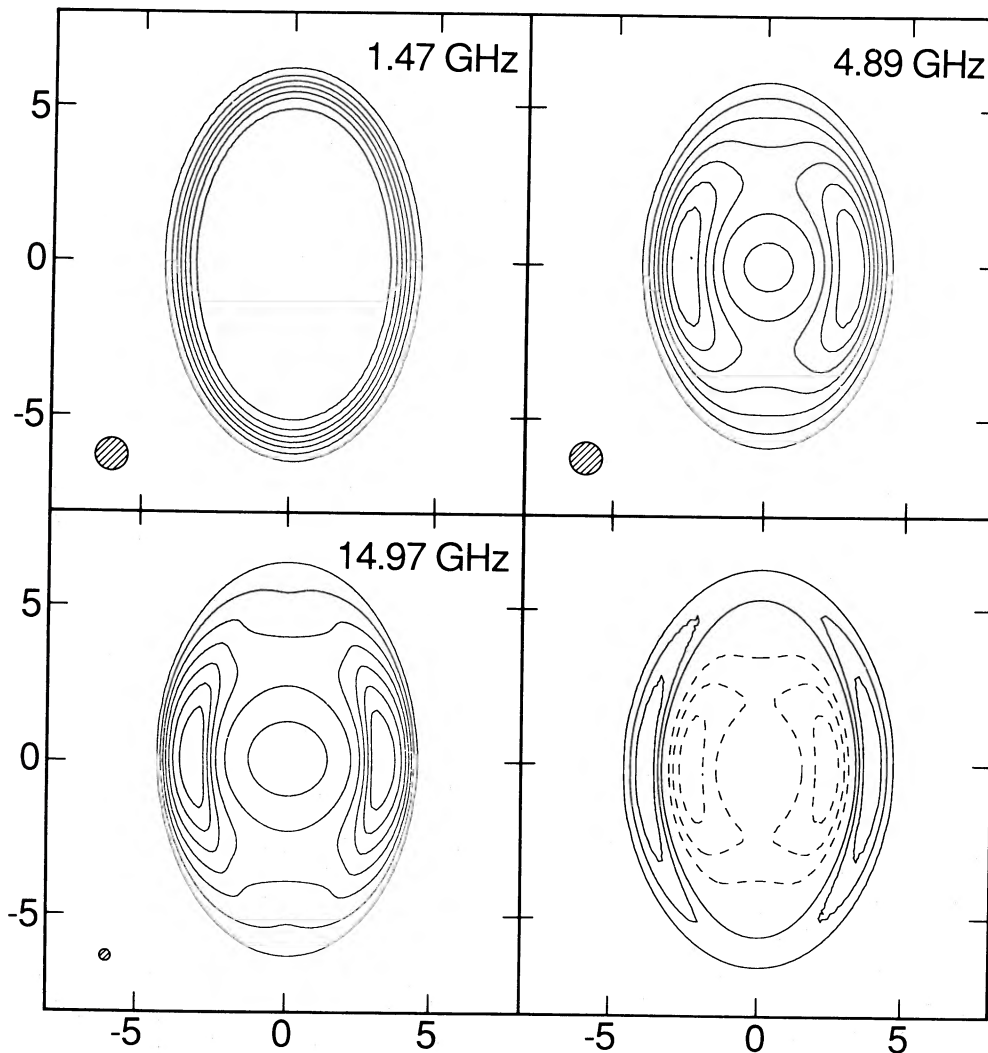[a] Baars *et al.* 1977.

[b] Basart and Daub 1987.

FIG. 5.—Model maps of NGC 7027. See text for details. (*upper left*) 1.465 GHz, with a resolution of 1″.5. (*upper right*) 4.885 GHz, with a resolution of 1″.05. (*lower left*) 14.965 GHz, with a resolution of 0″.35. (*lower right*) Difference map resulting from expansion of the nebula. The bulk motion on the minor axis was 80 mas at the outer edge of the nebulae and the ionization front advanced a further 59 mas along the minor axis. All maps have linear contours. The shaded ellipses show the FWHM beam areas.

<div align="center">

300

</div>

This asymmetry probably indicates that the ends of the nebula are hotter than the center, since the northern end is pointing toward us (Masson *et al.* 1985; Basart and Daub 1987). Second, the major axis is not sufficiently limb-brightened at 14.965 GHz. This is probably due to our choice of gas density as the variable which produces the reduction of emission away from the central star. Reduction of shell thickness on the major axis of the nebula can also give an appropriate flux variation, but with stronger limb brightening. The increase of temperature toward the ends of the nebula will also have a small effect in the direction of reducing emission. Probably there is a modest reduction in density towards the poles of the nebula, accompanied by a substantial decrease in the thickness of the walls. Substantial further physical modeling would be required to investigate this.

V. MODELING THE EXPANSION

Armed with a reasonably accurate model of the nebular structure, we now proceed to investigate its evolution. The largest effect is due to the expansion motion of the gas, which increases the size of the nebula. In addition, as the gas density drops, the ionization front will move ahead into the neutral gas, producing a greater change than that due to bulk motion alone. We assume that the density of the nebular gas falls as f^{-3} during the expansion, where f is the expansion factor. The volume emissivity therefore falls as f^{-6}, but the total radio emission is unchanged since the decrease is compensated by emission from the freshly ionized gas at the outside of the shell. The position of the ionization front depends also on the ionizing luminosity of the central star. If this luminosity increases or decreases, the nebula will expand or contract independently of the bulk motion. Such luminosity changes are, however, reflected in the optically-thin radio flux. We have combined the 1967 measurement by Pauliny-Toth and Kellerman (1969) with recent special VLA observations (R. Perley, private communication) to estimate the flux variation. These data are plotted in Figure 6. The observations were corrected to a common frequency using a spectral index of 0.4, estimated from the spectrum presented by Harris and Scott (1976), and adjusted to the scale of Baars *et al.* (1977). The best fitting line plotted in Figure 6 has a slope of -4.6 ± 4.6 mJy yr^{-1}. Another complication is the pressure of the gas inside the hollow nebula. If the pressure inside the shell changes, the density of the ionized gas will also change, as the gas expands into the central cavity or is further compressed. However, this would be compensated by an opposite motion of the ionization front and should therefore have only a small net effect on the mean size of the nebula. Measurement at higher resolution should be able to resolve the differential expansion between the inner and outer boundaries of the nebular shell. The form of the difference maps suggests that the axial ratio of the nebula remains approximately constant, with the gas moving outwards at a uniform velocity along the minor axis, and at a larger velocity in the polar direction, as found by Roelfsma *et al.* (1988). In the model calculations, we therefore assume a self-similar expansion and increase all dimensions by a factor f. To account for the excess motion of the ionization front, the outer boundary of the nebula is then adjusted to maintain a constant high-frequency radio flux. After expanding the nebular model, a difference map (Fig. 5 [*lower right*]) was computed for comparison with the maps in Figure 1.

The expansion motions were calculated from the model maps in the same way as was done for the observations. The calculated motion was greater than the bulk motion of the gas but significantly less than the motion of the ionization front. In Table 2, we have tabulated for each model a correction factor, which is the ratio of the bulk motion at the outer edge of the ionized region to the motion calculated from the model difference maps. For the best-fitting model, the correction factor is 0.87. Applying this to the measurements presented in § III, we deduce that the bulk motion of gas along the minor axis of NGC 7027 is 3.8 ± 0.3 mas yr^{-1}, where the quoted uncertainty
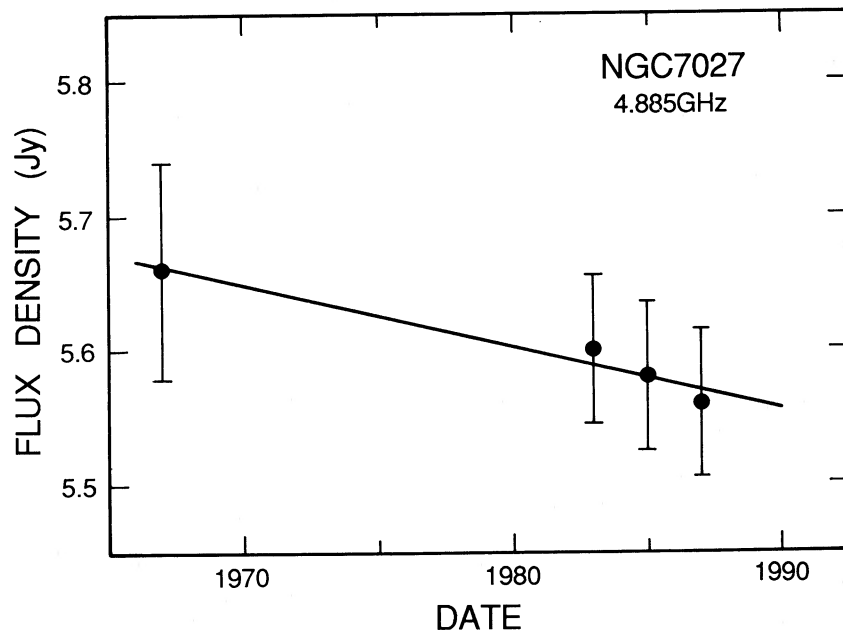

FIG. 6.—Flux density history of NGC 7027. The sources of the data are given in the text. All data have been corrected to the flux density scale of Baars *et al.* (1977) and adjusted to a frequency of 4.885 GHz based on the spectrum presented by Harris and Scott (1976).

includes only the measurement error. The range of correction factors in Table 2 suggests that the modeling contributes a further 5% uncertainty.

A correction must be made for the decrease in ionizing luminosity indicated by the small flux decrease at 5 GHz. Simulation of this effect based on the 30° model shows that the motion must be increased by $(0.47 \pm 0.47) \times 0.87$ mas yr^{-1}. The best estimate of the physical gas motion is then 4.2 ± 0.6 mas yr^{-1}, where the quoted error includes modeling and measurement uncertainties.

The velocity field of the ionized gas in the nebula is not well-determined, although it is known that the radial velocity varies along the major axis in a way consistent with the assumed expansion (Atherton et al. 1979; Roelfsma et al. 1988). In the self-similar model presented here, it is implicitly assumed that the nebular material is moving faster along the major axis, as suggested by the shape and the observations. For comparison with the angular expansion measurement we need only the velocity on the minor axis. Masson et al. (1985) have discussed the velocity field in the neutral gas and have shown that the velocity is isotropic with a value of 16.5 km s^{-1}. This is therefore a lower limit to the velocity of the ionized gas. A more direct estimate of the velocity of the ionized gas can be found by studying emission lines from the ionized gas itself, at the center of the nebular image. The recombination line observations of Roelfsma et al. (1988) do not have enough sensitivity to detect emission except in the limbs of the nebula, but the O [III] observations of Atherton et al. (1979) do have sufficient sensitivity. Figure 6b of the latter paper clearly shows double-peaked profiles resulting from the detection of gas at the front and back of the shell. In this case, the expansion velocity should be half the separation of the peaks, or 17.5 ± 1.5 km s^{-1}. Since the differentially expanding nebula is inclined to the line of sight, this value is likely to overestimate the equatorial expansion velocity, but the lower limit, given by the neutral gas velocity, is within the assumed uncertainty. We therefore adopt a value of 17.5 ± 1.5 km s^{-1} for the minor axis velocity. This is a lower velocity than we adopted in Paper I, where the value was based on the maximum velocity of the ionized gas. Although larger velocities are present in the emission from the nebula, it is clear from the data of Atherton et al. (1979) that they are due to systematic velocity shifts along the major axis.

Combining this velocity with the bulk motion of 4.2 mas yr^{-1}, we calculate that the distance to the nebula is 880 ± 150 pc. Despite the considerably improved model used here, the error is no better than the estimate given in Paper I. Paradoxically, this is due to the improved model itself, in which the thick ionized shell raises the importance of effects such as variations in the central star's luminosity. We estimate that uncertainties in the modeling amount to 10%, including velocity assumptions. Errors in the measurements contribute another 8%. The largest source of error is due to the changing flux density, which contributes another 11%, for a combined total of 17%. The new estimate of the distance, 880 ± 150 pc, agrees well with the provisional value of 940 ± 150 pc given in Paper I, and is consistent with the previous work summarized by Pottasch et al. (1982). Although the recognition that the walls of the nebula are quite thick had the effect of increasing the calculated distance, this was compensated by the downward revision of the velocity and by the correction due to flux changes.

In the future it is likely that the error can be reduced to 10% if careful flux monitoring, which is already in progress at the

VLA (R. Perley, private communication), is combined with measurements of the source structure over longer time intervals. At that point the limiting error will be set by modeling. However, further observations, particularly at high resolution, will also improve the models. It should be possible to measure independently the expansion of the inner and outer edges of the nebula. This would be a particularly interesting measurement for nebular models, since it would give valuable insight into the behavior of the high-temperature gas believed to provide the internal pressure (e.g., Kahn and West 1985). Better signal-to-noise ratio will also permit measurements along the major axis, again giving important information on the evolution of the source. Finally, the flux density measurements will trace the evolution of the central star as it cools to a white dwarf.

VI. DISCUSSION

The modeling of NGC 7027 and the determination of its distance permit an assessment of the age of the nebula and the evolutionary status of the central star. If, as argued above, the material on the minor axis has maintained a nearly constant velocity v, since it left the vicinity of the central star, the age of the nebula is simply r/v, where r is the inner minor radius, giving a value of ~ 600 yr. Since the flux from the central star cannot be measured directly, the total luminosity of the nebula is uncertain. However, a good lower limit is given by the observed infrared luminosity, which can be calculated from the data of Moseley (1980) as 2.1×10^{30} W, or $5.5 \times 10^3 L_\odot$. Pottasch (1984) estimates that the total luminosity is a factor of 3.5 times greater, or $2 \times 10^4 L_\odot$. These values place the central star of NGC 7027 on the horizontal part of the evolutionary track (cf. Pottasch 1984), near the point at which it should begin a rapid decline in luminosity and temperature. The present constancy of the flux density indicates that the decline has not started, but, within the next 1000 yr, the luminosity of the central star should drop by a factor of 10, with a corresponding decrease in nebular emission. The small decrease in flux density found here does not necessarily indicate that the luminosity of the central star is decreasing, since the radio flux density is proportional to the number of ionizing photons, which should decrease slightly as the temperature of the star increases at constant luminosity.

One important feature of the structure of NGC 7027 is the hollow center, which must be maintained by some source of pressure. The radiation pressure, $P_{\rm rad}$, on the shell is given approximately by

$$P_{\rm rad} = \frac{L}{4\pi r^2 c},$$

where L is the luminosity of the central star and r is the distance from the star. There is an additional contribution from Lyman-continuum photons which are scattered backward and forward across the shell, but this is not a large correction since almost all of these photons must be absorbed by dust (Pottasch 1984). At the inner surface on the minor axis, the electron density from our model is 7×10^4 cm^{-3}, and the corresponding pressure is 2.8×10^{-8} Pa. If the total luminosity is $2 \times 10^4 L_\odot$ and all of the momentum is transferred to the nebular gas, the radiation pressure is 1.8×10^{-8} Pa, insufficient to confine the ionized gas, although the effect is not negligible. Away from the minor axis, the radiation pressure falls faster than the gas pressure so the deficiency becomes larger. Therefore radiation

pressure alone cannot maintain the hollow center of the shell. A wind from the central star could be responsible (Kwok, Purton, and Fitzgerald 1979), although there is no direct evidence for such a wind in NGC 7027, since the central star itself has not been detected. As noted above, the measurement of temporal changes in the source structure will provide valuable information to constrain such wind models.

VII. CONCLUSIONS AND FUTURE PROSPECTS

We have analyzed high-resolution radio maps of NGC 7027 to derive a new model which is consistent with ionization by a single central source. The observations are well fitted by gas in a relatively thick ($\Delta r/r \sim 0.3$), elongated, ellipsoidal shell tilted at $30°$ to the line of sight. Despite the thickness of the shell, the center of the nebula has low emission because the central line of sight passes through parts of the shell which are relatively distant from the central star and receive a low ionizing flux. The gas temperature is 14,500 K, and the equatorial electron density is 7×10^4 cm^{-3}; the polar regions probably have slightly higher temperature and lower gas density than the equator.

We have measured the expansion of the nebula, based on three epochs of VLA data between 1982 and 1986, confirming the result initially presented by Masson (1986). Comparison with model calculations shows that the material on the minor axis of the nebula is moving at a steady rate of 4.2 mas yr^{-1}. Combined with a velocity of 17.5 km s^{-1}, this gives a distance to the nebula of 880 $\pm$ 150 pc, in good agreement with earlier estimates (Masson 1986; Pottasch et al. 1982). The uncertainty of 17% is largely due to possible changes in the central star and to errors in modeling of the nebula; it should be significantly reduced by further observations.

It is important to estimate the range of application of the method presented here. The signal-to-noise ratio in the present measurements is so large that the expansion of NGC 7027 could easily have been measured out to a distance of several kpc. At the distance of the Galactic center, the A array would be needed for higher resolution, but the distance could be measured with a worthwhile accuracy (30%) in as little as 10 yr. From the compilation of Pottasch (1984), we estimate that about 25 nebulae have mean surface brightness greater than 20 mJy beam^{-1} for the B array of the VLA, about 10% of the peak brightness of NGC 7027. Since our measurements of NGC 7027 were limited by systematic errors rather than by random noise, it should be possible to measure these objects with a standard deviation of about 2 mas. With a time interval of 5 yr, the standard deviation of the angular expansion measurement should be 0.4 mas yr^{-1}, corresponding to a distance of 8 kpc for a typical velocity of 20 km s^{-1}. A further 19 objects are listed as having brightness greater than 5 mJy beam^{-1} and should be measurable over a period of one to two decades. Some of the nebulae are southern objects and will need the Australia Telescope, while others are very compact and will require higher frequencies or larger configurations of the VLA. Against this must be set the fact that the list given by Pottasch is not exhaustive. In summary it appears that, within a relatively modest time of one to two decades, it will be possible to measure distances to several dozen planetary nebulae; many of those distances will be available in a much shorter time. We have already made measurements to find the distances to the nebulae BD $+30°3639$ and NGC 6572 (Masson 1989b).

A number of other objects are expected to show proper motions of a few mas yr^{-1}. Among these are compact H II regions, whose ages and evolution are poorly understood at present. Observations are already under way to measure the expansion of W3(OH). The angular expansion will immediately give a dynamical age for the region, and hence for the central star, while detailed study may shed light on the evolution of the region. Another structure which should have proper motions of about 5 mas yr^{-1} is the Galactic center. The ionized gas within 1 pc of the center may be orbiting, infalling, outflowing, or displaying some combination of these motions (e.g., Serabyn and Lacy 1985). Although the signals are weaker, an excellent point source is available for calibration and this experiment should provide a definitive discrimination between infall and outflow.

REFERENCES

Atherton, P. D., Hicks, T. R., Reay, N. K., Robinson, G. J., Worswick, S. P., and Phillips, J. P. 1979, Ap. J., 232, 786.
Baars, J. W. M., Genzel, R., Pauliny-Toth, I. I. K., and Witzel, A. 1977, Astr. Ap., 61, 99.
Basart, J. P., and Daub, C. T. 1987, Ap. J., 317, 412.
Harris, S., and Scott, P. F. 1976, M.N.R.A.S., 175, 371.
Kahn, F. D., and West, K. A. 1985, M.N.R.A.S., 212, 837.
Kwok, S., Purton, C., and Fitzgerald, P. 1979, Ap. J. (Letters), 219, L125.
Masson, C. R. 1986, Ap. J. (Letters), 302, L27 (Paper I).
———. 1989a, in preparation.
———. 1989b, in preparation.
Masson, C. R., et al. 1985, Ap. J., 292, 464.
Moseley, H. 1980, Ap. J., 238, 892.
Mufson, S. L., Lyon, J., and Marionni, P. A. 1975, Ap. J. (Letters), 201, L85.
Pauliny-Toth, I. I. K., and Kellerman, K. 1969, A.J., 73, 953.

Phillips, J. P., Reay, N. K., and Worswick, S. P. 1980, M.N.R.A.S., 193, 231.
Pottasch, S. R. 1984, in IAU Symposium 103, Planetary Nebulae, ed. D. R. Flower (Dordrecht: Reidel), p. 215.
Pottasch, S. R., Goss, W. M., Arnal, E. M., and Gathier, R. 1982, Astr. Ap., 106, 229.
Roelfsma, P. R., Goss, W. M., Pottasch, S. R., and Zijlstra, A. 1988, Astr. Ap., in press.
Salpeter, E. 1978, in IAU Symposium 76, Planetary Nebulae: Observations and Theory, ed. Y. Terzian (Dordrecht: Reidel), p. 333.
Schneider, S. E., and Terzian, Y. 1983, Ap. J. (Letters), 274, L61.
Schwab, F. 1980, International Optical Computing Conference, Book 1, ed. W. T. Rhodes (Proc. SPIE, Vol. 231), p. 18.
Scott, P. F. 1973, M.N.R.A.S., 161, 35.
Serabyn, E., and Lacy, J. H. 1985, Ap. J., 293, 445.

COLIN R. MASSON: Caltech 405-47, Pasadena, CA　91125